Critical currents in weakly textured MgB_2: Nonlinear transport in anisotropic heterogeneous media

M. Eisterer,[1] W. Häßler,[2] and P. Kováč[3]
[1]*Atominstitut, Vienna University of Technology, 1020 Vienna, Austria*
[2]*Institute for Metallic Materials, IFW Dresden, D-01171 Dresden, Germany*
[3]*Institute of Electrical Engineering, Slovak Academy of Sciences, Bratislava, Slovakia*
(Received 15 October 2009; published 17 November 2009)

A model for highly nonlinear transport in heterogeneous media consisting of anisotropic particles with a preferred orientation is proposed and applied to the current transport in weakly textured magnesium diboride, MgB_2. It essentially explains why, unlike in conventional superconductors, a significant macroscopic anisotropy of the critical currents can be induced by the preparation of MgB_2 tapes. The field and angular dependence of the critical current is calculated for various degrees of texture and compared to experimental data.

DOI: 10.1103/PhysRevB.80.174516 PACS number(s): 74.70.Ad, 74.25.Sv, 74.81.Bd, 81.40.Ef

I. INTRODUCTION

The critical current in polycrystalline MgB_2 is a particular example of nonlinear transport in heterogeneous media.[1] The intrinsic upper critical field anisotropy results in different critical current densities in differently oriented grains, when a magnetic field is applied.[2] The problem was solved by integration of the (local) current densities over the percolation cross section, for which the distribution function of the local critical currents has to be known. Although the local currents can be described by standard pinning models,[3] the resulting macroscopic currents are significantly altered. The field dependence of the critical current increases and the current becomes zero well below the upper critical field.[2]

In the present paper, a heterogeneous and macroscopically anisotropic system is considered, i.e., the distribution function of the relevant transport property (e.g., the critical current density J_c) depends on its orientation. This is realized in weakly (or partially) textured MgB_2 and explains the J_c anisotropy,[4–12] which can exceed the *intrinsic* anisotropy of MgB_2 (5–6)[13] by orders of magnitude. The J_c anisotropy can be induced by some preparation techniques of MgB_2 tapes, which was impossible in the conventional superconductors NbTi and Nb_3Sn since they are intrinsically isotropic. On the other hand, high temperature superconductors must be highly textured for enabling large transport currents. Thus, MgB_2 is the first superconductor needing a model for partial texture as description. The distribution function of J_c in MgB_2 will be derived in the following, but it is straightforward to apply the model to any other highly nonlinear transport phenomena in anisotropic heterogeneous media.

II. EXPERIMENTAL

Powders of magnesium (Goodfellow, 99.8%) and amorphous boron (Starck, 95%–97%) were milled together for 50 h at 250 rpm in a planetary ball mill (Retsch PM 4000) under protecting argon atmosphere. The powder was filled into iron tubes and deformed by swaging and rolling into tapes and heat treated. One tape was doped with nanostructured carbon (99.999%), which had been added to the precursor powders before milling (nominal $MgB_{1.87}C_{0.13}$).

The critical current was measured by direct transport measurements in liquid helium. The texture was characterized by measuring rocking curves of the MgB_2(002) reflection using high energy synchrotron x-ray (E=77.5 keV) diffraction. Details of all measurements and the sample preparation are given elsewhere[14] since we will focus on the proposed model, while the experimental data are used for comparison.

III. MATHEMATICAL MODEL

The macroscopic critical current density in anisotropic polycrystalline superconductors (or any other transport property in heterogeneous media, which hardly depends on the driving force) can be calculated from[2]

$$J_c^{\mathrm{macro}} = \int_0^{J_{\max}} \left(\frac{p(J) - p_c}{1 - p_c} \right)^{1.76} dJ. \tag{1}$$

The percolation threshold p_c is defined as the minimum fraction of superconducting grains for a continuous current path. $p(J)$ is the fraction of grains with a (local) J_c exceeding J and $J_{\max}$ is given by the condition $p(J_{\max})=p_c$. The field dependence of the (local) critical currents is assumed to follow the well established model for grain boundary pinning[3]

$$J_c^{\mathrm{local}}(B) \propto \frac{\left(1 - \frac{B}{B_{c2}}\right)^2}{\sqrt{B}} \tag{2}$$

for $B < B_{c2}$ and $J_c^{\mathrm{local}}=0$ otherwise. For the sake of simplicity, any difference between the upper critical field, B_{c2}, and the irreversibility field, B_{irr}, is neglected. The angular dependence of the critical current is modeled by the scaling approach proposed by Blatter *et al.*,[15] i.e., B is multiplied by $\sqrt{\cos^2\theta + \gamma^{-2}\sin^2\theta}$, where γ denotes the anisotropy of the upper critical field B_{c2}^{ab}/B_{c2}^{c} and θ the angle between the applied magnetic field and the crystallographic c axis; thus, B_{c2} in Eq. (2) corresponds to B_{c2}^{c}, the upper critical field for $B \| c$.

The angular distribution of the grain orientation, $p_a(\theta)$, is needed for calculating $p(J)$. Each grain is represented by a point on the surface of the unit sphere ($\vec{r}$ in Fig. 1), which corresponds to the orientation of its c axis. The density of

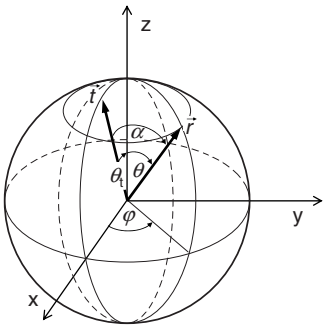

FIG. 1. Spherical coordinate system. The magnetic field is assumed to be parallel to the z axis. θ and φ denote the polar and azimuthal angle, respectively. The preferred orientation (texture) of the grains lies in their c axis parallel to $\vec{t}$.

these points, $f_a(\theta,\varphi)$ is per definition constant for a random grain orientation. The number of grains with a polar angle equal to or above θ is obtained from integration of $f_a(\theta,\varphi)$ over the corresponding surface area

$$p_a(\theta) = \int_{\theta}^{\pi/2} \int_{0}^{2\pi} f_a(\theta',\varphi) d\varphi \sin\theta' d\theta', \tag{3}$$

which reduces to $2\pi f_a \cos\theta$ for constant f_a. The sine of θ' is the radius of the circle, along which the integration over φ is carried out (cf. Fig. 1). Due to the symmetry of the problem, the integration can be restricted to the upper half of the unit sphere. The relative fraction of such oriented grains is obtained by setting $f_a = 1/2\pi$ (the surface of the unit sphere is 4π). This leads to $p_a(\theta) = \cos\theta$ and to the correct result $p_a(0) = 1$ for a random grain orientation.

Partial texture can be introduced by a varying density $f_a(\theta,\varphi)$. For uniaxial texture, the density becomes independent of the azimuthal angle (φ), if the preferred orientation of the grains' c axis is assumed to be parallel to the z axis. A natural choice for the variation along the polar angle is a Gaussian (or normal) distribution

$$f_a(\theta,\varphi) \propto \exp\left(-\frac{\theta^2}{2\alpha_t^2}\right), \tag{4}$$

with standard deviation α_t. The proper normalization is obtained as above by integration of $f_a(\theta,\varphi)$ over half the unit sphere and $p_a(\theta)$ can then be calculated from Eq. (3). The chosen density function was confirmed by synchrotron x-ray diffraction with $\alpha_t = 29.3°$,[14] but it is straightforward to use any other distribution.

If the direction of the applied magnetic field is chosen as the z axis, the preferred orientation of the grains' c axis is in general not parallel to this direction. The situation is illustrated in Fig. 1. The preferred orientation is defined by $\vec{t}$ with spherical coordinates $(\theta_t, \varphi = 0)$. The angle, α, between $\vec{t}$ and an arbitrary direction $\vec{r}$ is given by

$$\cos\alpha = \mathrm{abs}(\sin\theta\cos\varphi\sin\theta_t + \cos\theta\cos\theta_t). \tag{5}$$

The density function $f_a(\theta,\varphi)$ is obtained from Eq. (4) by replacing θ by α. It depends on the polar and azimuthal angle

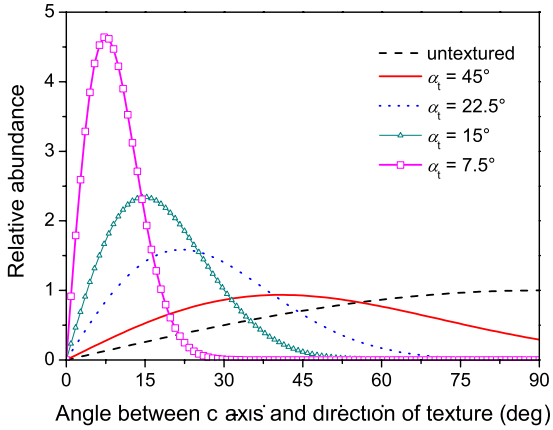

FIG. 2. (Color online) Grain orientation with respect to the direction of partial texture. The maximum shifts continuously from the perpendicular orientation (90°) for random grain orientation to zero in the limit of perfect texture ($\alpha_t \to 0$).

and the two dimensional integration (3) has to be calculated numerically.

At fixed magnetic field, $p(J)$ can be calculated from $p_a(\theta)$, since J_c^{local} depends monotonically on θ. Finally, J_c^{macro} is obtained by numerical evaluation of integral (1).

IV. RESULTS AND DISCUSSION

The relative abundance of grains, whose c axis is tilted by an angle θ from the direction of the texture $\vec{t}$, is obtained by integration of $f_a(\theta,\varphi)$ over φ, which is the negative derivative of $p_a(\theta)$. It is plotted in Fig. 2 for various angles α_t, which characterize the degree of texture. With increasing texture, the maximum shifts from $\pi/2$ for randomly oriented grains to smaller angles. (In the limit $\alpha_t \to 0$ (perfect texture), the distribution function becomes a δ function.) For weak texture, the majority of grains is *not* oriented with the c axis close to the direction of the uniaxial texture, but the fraction of grains with perpendicular orientation is reduced and becomes negligible for $\alpha_t \approx 25°$.

The influence of partial texture on the field dependence of the critical currents is shown in Fig. 3. The two panels refer to different anisotropies; 5 is typical for clean MgB_2, 3 for moderately dirty MgB_2.[13] The magnetic field is normalized by B_{c2}^{ab}. B_{c2}^{c} is $1/\gamma$ (0.2 and $0.\dot{3}$). The percolation threshold was fixed to 0.25, which is an average value in polycrystalline MgB_2.[2,4,16,17] The central bold line was calculated for the untextured material, the graphs below and above this line refer to the parallel ($\theta_t = 0°$) and perpendicular ($\theta_t = 90°$) field orientation. With decreasing α_t (increasing texture) the critical current becomes more anisotropic and the data converge much faster to the limiting case of perfect texture (thin solid lines) for the parallel orientation, where the difference between perfect and partial texture becomes small at $\alpha_t \sim 20°$. The J_c anisotropy decreases with decreasing γ but the qualitative behavior is the same in both panels.

The angular dependence of the critical currents is plotted in Fig. 4. The assumed texture is stronger in the lower panel, the anisotropy ($\gamma = 5$) and p_c (0.25) were kept constant. At

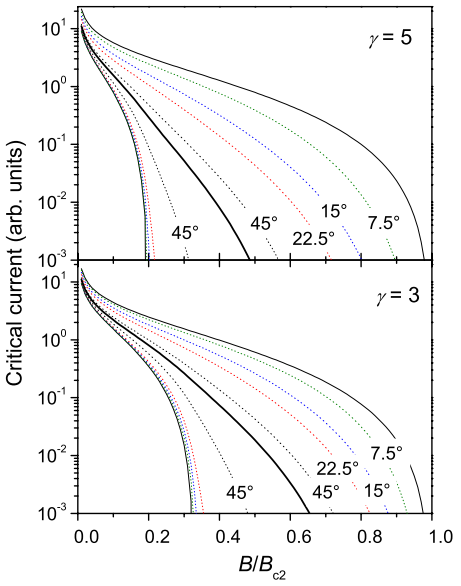

FIG. 3. (Color online) Influence of partial texture on the critical currents. The given angles refer to α_t. The central bold lines represent untextured MgB_2. The dotted lines below and above the bold lines correspond to the field orientation parallel and perpendicular to the direction of texture. The limiting curves represent perfect texture.

low magnetic fields, the J_c anisotropy is small for the more weakly textured material (1.2 at $B/B_{c2}=0.01$), but increases with texture (to $\sqrt{\gamma}$ for $B\to 0$ for perfect texture, line graph in Fig. 4). The J_c anisotropy monotonically increases with magnetic field until it diverges for any $\alpha_t<\infty$, when the currents reduce to zero in the parallel orientation ($\theta_t=0°$). This was observed experimentally.[5–7] (Note that $\vec{t}$ is perpendicular to the surface of MgB_2 tapes, hence the parallel orientation

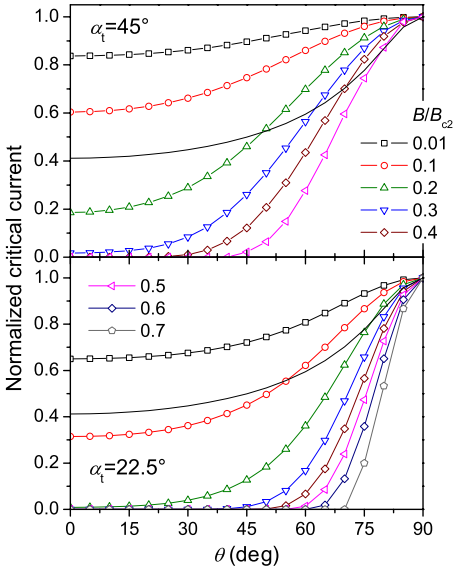

FIG. 4. (Color online) Angular dependence of the critical current. $\gamma=5$ and $p_c=0.25$ are assumed. The texture is stronger in the lower panel. The graphs without symbols refer to perfect texture (anisotropic scaling approach) (Ref. 15) at $B/B_{c2}=0.01$. The critical current anisotropy increases with field.

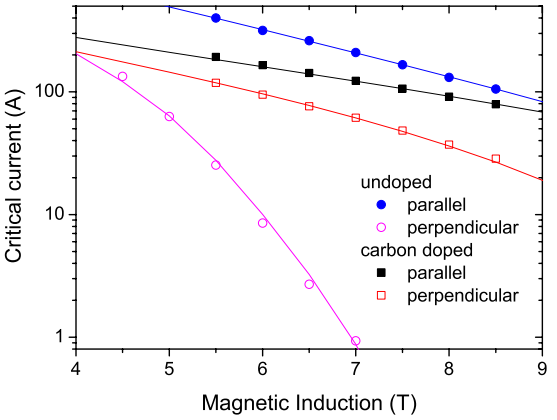

FIG. 5. (Color online) The model (line graphs) successfully describes the measured critical currents (symbols) for both main field orientations.

($\theta_t=0°$) corresponds to the field perpendicular to the tape.) At fixed γ, p_c, and α_t, the J_c anisotropy is only a function of the reduced magnetic field $b=B/B_{c2}$, which explains its temperature dependence at fixed magnetic field: b increases with temperature, since B_{c2} decreases.

Experimental data (symbols) for the critical current are compared to the prediction of the present model (line graphs) in Figs. 5 and 6. The agreement is excellent, given the numerous assumptions/simplifications (pure grain boundary pinning,[3] anisotropic scaling,[15] Gaussian distribution, etc.). The correct choice of the (unknown) parameters is difficult, since a 5 parameter fit (B_{c2}, γ, α_t, p_c, and a constant prefactor, I_{c0}) does not lead to significant results. Therefore, p_c was fixed to 0.25 and α_t to 29.3°.[14] The remaining parameters were adapted to fit the experimental $J_c(B)$ data for both field orientations simultaneously. $B_{c2}=23.2(20.5)$ T, $\gamma=4.05(1.8)$, and $I_{c0}=2840(860)$ A were chosen for the undoped (doped) tape. The parameters of the doped tape ($T_c=29.5$ K) agree fairly well with results on a carbon doped (9.5%) single crystal with a similar $T_c=30.6$ K,[18] where γ slightly below 2 and $B_{c2}(0)=25$ T (suggesting a value of around 21 T at 4.2 K) were reported. The higher anisotropy of the undoped tape is expected from its higher T_c (34.4 K) and also B_{c2} tends to decrease for transi-

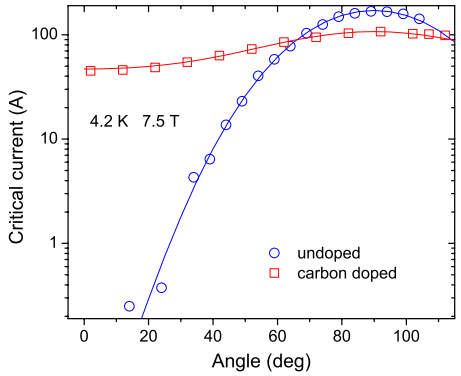

FIG. 6. (Color online) Calculated (lines) and experimental (symbols) angular dependence of the critical currents at 7.5 T in liquid helium.

tion temperatures of below ~32 K.[13] The larger I_{c0} of the undoped tape confirms that carbon doping decreases pinning[13,19] and the connectivity.

A discrepancy between experimental and calculated data was found at small currents (<1 A, θ_t=0°, not shown in Fig. 5), which might be a consequence of the finite voltage during transport measurements (1 μV cm^{-1}), which allows small currents passing normal conducting grains. Such normal currents are excluded in the present model and might add a significant contribution at small critical currents (by connecting otherwise disconnected superconducting clusters), but they can certainly be neglected at high critical currents. On the other hand, the discrepancy could also result from inhomogeneities, texture gradients,[6,8] or a different distribution function of the grain orientation. Note that the Gaussian distribution function was also used in Ref. 6 and an even higher degree of texture ($\alpha_t \sim 20°$ and ~25° according to our definition) was found near the sheath of cold rolled *ex situ* tapes, decreasing toward the center.

The angular dependence of J_c was calculated with the same parameters, which describe the data very well. However, without a knowledge of the anisotropy the texture (α_t) cannot be derived due to the mutual influence of α_t and γ.

V. CONCLUSIONS

The proposed model successfully describes the field and angular dependence of the critical currents in weakly textured MgB_2 tapes and explains the large difference between the *intrinsic* and *extrinsic* (J_c) anisotropy.

ACKNOWLEDGMENTS

The authors wish to thank Harald Weber for critically reading the manuscript and for his valuable comments. We are grateful to Asger Abrahamsen for his synchrotron measurements and fruitful discussions.

[1] M. Sahimi, Phys. Rep. **306**, 213 (1998).
[2] M. Eisterer, M. Zehetmayer, and H. W. Weber, Phys. Rev. Lett. **90**, 247002 (2003).
[3] D. Dew-Hughes, Philos. Mag. **30**, 293 (1974).
[4] V. Beilin, I. Lapides, M. Roth, E. Dul'kin, E. Mojaev, A. Gerber, and O. Riss, J. Appl. Phys. **100**, 043903 (2006).
[5] P. Kováč, T. Melišek, and I. Hušek, Supercond. Sci. Technol. **18**, L45 (2005).
[6] P. Lezza, R. Gladyshevskii, V. Abächerli, and R. Flükiger, Supercond. Sci. Technol. **19**, 286 (2006).
[7] P. Kováč, I. Hušek, E. Dobročka, T. Melišek, W. Haessler, and M. Herrmann, Supercond. Sci. Technol. **21**, 015004 (2008).
[8] X. Song, S. E. Babcock, C. B. Eom, D. C. Larbalestier, K. A. Regan, R. J. Cava, S. L. Bud'ko, P. Canfield, and D. K. Finnemore, Supercond. Sci. Technol. **15**, 511 (2002).
[9] G. Grasso, A. Malagoli, D. Marré, E. Bellingeri, V. Braccini, S. Roncallo, N. Scati, and A. S. Siri, Physica C **378-381**, 899 (2002).
[10] H. Kitaguchi and H. Kumakura, Supercond. Sci. Technol. **18**, S284 (2005).
[11] P. Lezza, R. Gladyshevskii, C. Senatore, G. Cusanelli, H. L. Suo, and R. Flükiger, IEEE Trans. Appl. Supercond. **15**, 3196 (2005).
[12] G. Serrano, A. Serquis, L. Civale, B. Maiorov, M. T. Malachevsky, and C. Ayala, J. Phys.: Conf. Ser. **97**, 012129 (2008).
[13] M. Eisterer, Supercond. Sci. Technol. **20**, R47 (2007).
[14] W. Häßler *et al.* (unpublished).
[15] G. Blatter, V. B. Geshkenbein, and A. I. Larkin, Phys. Rev. Lett. **68**, 875 (1992).
[16] A. Yamamoto, J.-i. Shimoyama, K. Kishio, and T. Matsushita, Supercond. Sci. Technol. **20**, 658 (2007).
[17] M. Eisterer, J. Emhofer, S. Sorta, M. Zehetmayer, and H. W. Weber, Supercond. Sci. Technol. **22**, 034016 (2009).
[18] C. Krutzler, M. Zehetmayer, M. Eisterer, H. W. Weber, N. D. Zhigadlo, J. Karpinski, and A. Wisniewski, Phys. Rev. B **74**, 144511 (2006).
[19] J. H. Kim, S. X. Dou, S. Oh, M. Jerčinović, E. Babić, T. Nakane, and H. Kumakura, J. Appl. Phys. **104**, 063911 (2008).